CRL4[VprBP] E3 ligase promotes monoubiquitylation and chromatin binding of TET dioxygenases

Tadashi Nakagawa[#1], **Lei Lv**[#1], **Makiko Nakagawa**[1], **Yanbao Yu**[2], **Chao Yu**[3], **Ana C. D'Alessio**[1], **Keiko Nakayama**[4], **Heng-Yu Fan**[3], **Xian Chen**[2], and **Yue Xiong**[1,2,*]

[1]Lineberger Comprehensive Cancer Center, University of North Carolina at Chapel Hill, NC 27599, USA

[2]Department of Biochemistry and Biophysics, University of North Carolina at Chapel Hill, NC 27599, USA

[3]Life Sciences Institute, Zhejiang University, Hangzhou 310058, China

[4]Division of Cell Proliferation, ART, Graduate School of Medicine, Tohoku University, Sendai 980-8575, Japan

[#] These authors contributed equally to this work.

SUMMARY

DNA methylation at the C-5 position of cytosine (5mC) regulates gene expression and plays pivotal roles in various biological processes. The TET dioxygenases iterative oxidation of 5mC, leading to eventual demethylation intermediate. Inactivation of TET enzymes causes multi-stage developmental defects, impaired cell reprogramming and hematopoietic malignancies. However, little is known about how TET activity is regulated. Here we show that all three TET proteins bind to VprBP and are monoubiquitylated by the VprBP-DDB1-CUL4-ROC1 E3 ubiquitin ligase (CRL4[VprBP]) on a highly conserved lysine residue. Deletion of *VprBP* in oocytes abrogated paternal DNA hydroxymethylation in zygotes. VprBP-mediated monoubiquitylation promotes TET binding to chromatin. Multiple recurrent TET2-inactivating mutations derived from leukemia target either the monoubiquitylation site (K1299) or residues essential for VprBP binding. Cumulatively, our data demonstrate that CRL4[VprBP] is a critical regulator of TET dioxygenases during development and in tumor suppression.

INTRODUCTION

5-methylcytosine (5mC) is a genomic modification that negatively regulates gene expression and is essential for diverse biological processes (Li, 2002; Wu and Zhang, 2014). 5mC patterning is established by DNA methyltransferase (DNMT) 3 and is maintained by

DNMT1, which methylates newly replicated DNA (Goll and Bestor, 2005). Once considered irreversible, the recent identification of the TET family of proteins (TET1, 2 and 3 in mammalian cells) has changed our view of 5mC stability (Tahiliani et al., 2009). TET proteins are α-ketoglutarate (α-KG)- and Fe(II)-dependent dioxygenases that catalyze three steps of iterative oxidation, first converting 5mC to 5-hydroxymethyl cytosine (5hmC), then 5hmC to 5-formyl cytosine (5fC), and finally 5fC to 5-carboxy cytosine (5caC). 5caC can be removed by DNA glycosylase TDG, resulting in 5-unmodified cytosine (He et al., 2011; Ito et al., 2011). Besides being an intermediate in demethylation, emerging data indicate that 5hmC is recognized by several chromatin factors and may directly contribute to gene regulation (Mellen et al., 2012; Yildirim et al., 2011).

Conditional zygotic deletion of *Tet3* blocks paternal-genome conversion of 5mC into 5hmC and results in multiple developmental defects, supporting a critical developmental role for TET enzymes (Gu et al., 2011). Tet1 depletion results in defective DNA demethylation in primordial germ cells and decreased expression of a subset of meiotic genes, leading to reduced female germ cells and fertility (Yamaguchi et al., 2012). During induced pluripotent stem cell (iPSC) reprogramming, TET1 and TET2 promote 5mC-to-5hmC conversion to facilitate imprint erasure and establish pluripotency in somatic cells (Costa et al., 2013; Doege et al., 2012; Piccolo et al., 2013). Pathologically, the *TET2* gene is frequently mutated in human hematopoietic malignancies of both myeloid, in particular acute myeloid leukemia (AML, ~15–20%), and lymphoid lineages, such as angioimmunoblastic T-cell lymphoma (AITL, ~30–40%) (Delhommeau et al., 2009; Quivoron et al., 2011; Tefferi et al., 2009). While the biological function and catalytic mechanism of TET enzymes are extensively investigated, little is known about their regulation.

The covalent attachment of ubiquitin to a substrate protein (ubiquitylation) is involved in most cellular processes (Glickman and Ciechanover, 2002). Ubiquitylation proceeds through sequential reactions promoted by a ubiquitin-activating enzyme (E1), a ubiquitin-conjugating enzyme (E2), and finally a ubiquitin ligase (E3) that binds substrates and determines specificity. Substrate modification with either a single ubiquitin or various lengths and linkages of ubiquitin chains enables substrate recognition by distinct ubiquitin-binding proteins, leading to specific biochemical consequences including degradation, translocation, and recruitment of other proteins. Cullin proteins, which comprise the largest family of E3s, form multiple cullin-ring ubiquitin ligase (CRLs) complexes that include a small RING protein, ROC1 or ROC2 (also known as RBX), which activates E2, and substrate recognition subunits. CUL4, conserved from yeast to humans, has two paralogs in mammalian cells, CUL4A and CUL4B. Both use damaged DNA binding protein 1 (DDB1) as a linker to interact with multiple *D*DB1-binding *WD*40 (DWD, also known as DCAF for *D*DB1 and *c*ullin *a*ssociated *f*actors) proteins that serve as substrate recognition subunits. The functions of CUL4 genes have been genetically linked to chromatin regulation (Jackson and Xiong, 2009). This report shows that VprBP/DCAF1, one of the strongest and most abundant binding partners of DDB1 (McCall et al., 2008), promotes monoubiquitylation of TET enzymes and their DNA binding.

RESULTS

VprBP binds the cysteine-rich, dioxygenase (CD) domain of TET

The C-terminal WD40 domain of VprBP binds to DDB1 and, through DDB1, interacts with CUL4 to assemble an active catalytic moiety while the N-terminal region is predicted to interact with substrates (McCall et al., 2008; Nakagawa et al., 2013). Thus, we established 293T cells stably expressing a FLAG-tagged VprBP deletion mutant that contains the N-terminal 909 amino acids (VprBP[N909]). We conducted an immunoprecipitation (IP) followed by mass spectrometric (IP-Mass spec) analysis in this cell line to identify proteins that specifically bind to the VprBP[N909] mutant (Figure 1A). The VprBP[N909] mutant does not contain the DDB1 binding domain, thus the association with CUL4 and the catalytic ROC1 RING finger subunit is disrupted, potentially trapping the binding of VprBP with its substrates. We identified a large number of potential VprBP-interacting proteins, including TET2 (Figure S1 and Table S1). Immunoblotting confirmed the retention of VprBP[N909] in TET2 immunoprecipitates and also demonstrated that full-length VprBP binds to TET2 (Figures 1A and 1E). To determine the VprBP binding region in TET2, we constructed several deletion mutants and found the C-terminal *cysteine-rich dioxygenase* (CD) domain of TET2 (CD2) to be primarily responsible for binding to VprBP (Figure 1B). Consistent with the high conservation of CD domains among TET paralogs, all three TET CD domains and full length TET proteins bound to VprBP in cells (Figures 1C and 1D). Catalytically inactive TET CDs also bound to VprBP (Figure 1C), suggesting that the catalytic activity is not involved in this binding. Importantly, endogenous TET proteins were readily detected in association with endogenous VprBP in mouse embryonic fibroblasts (MEFs), mouse embryonic stem (ES) cells and human monocytes (Figure 1E). An in vitro binding assay showed that VprBP, but not DDB1, directly binds to TET2-CD (Figure 1F). Together, these studies demonstrated that VprBP binds directly to all three TET proteins.

VprBP function is important for paternal DNA hydroxymethylation and zygotic development

To determine the functional significance of VprBP-TET interaction, the effect of *VprBP* deletion on 5hmC level in MEF cells was examined. Because *Vprbp* is essential for mouse embryo development and cell growth, we used a conditional *Vprbp* knockout mouse strain we previously created (McCall et al., 2008)-*VprBP[f]*. Here, expression of cre recombinase deletes a 2,358 bp genomic segment containing exons 7 and 8, which encodes 203 amino acid residues (residue Val172 to Ala374). *VprBP[f/f]* MEFs were infected with adenovirus-expressing Cre to effectively delete *VprBP* gene and abolish the expression of *VprBP* mRNA, but not affecting the expression of either Tet2 or Tet3 (Figure 2A). Deletion of VprBP gene caused substantial reduction of 5hmC, suggesting that the function of VprBP is important for TET activity (Figure 2A).

One critical function of TET family dioxygenases is TET3-catalyzed paternal genome hydroxymethylation in the zygote (Gu et al., 2011). To determine the physiological significance of CRL4[VprBP]-mediated TET activation, we next examined the role of VprBP in paternal genome DNA hydroxymethylation and zygotic development. *Vprbp[f/f]* were crossed with *Zp3*-Cre mice expressing the cre recombinase under the promoter of mouse

zona pellucida 3 gene (*Zp3*). This cross led to *Vprbp* knockout exclusively in the growing oocyte, prior to completion of the first meiotic division (Lewandoski et al., 1997). To determine the effects of oocyte *Vprbp* deletion on zygotic development, female *Vprbp*$^{f/f}$ and *Vprbp*$^{f/f}$;*Zp3-Cre* mice were superovulated, and embryos were examined microscopically. While the *Vprbp*$^{f/f}$ embryos developed to the 4-cell stage, the *Vprbp*$^{f/f}$;*Zp3-Cre* zygotes were arrested at the 1-cell stage and failed to start embryogenesis or cleavage (Figure 2B) which reveals a critical function of VprBP in zygotic development. Synchronously, VprBP was expressed at a readily detectable level in oocytes with an evident accumulation in the nucleus (Figure 2C). Efficient deletion of *VprBP* by *Zp3*-driven Cre was confirmed by immunohistochemistry (Figure 2C). This analysis showed a reproducible and partially penetrant developmental defect in a fraction of oocytes (Figure 2C and Figure S2). Notably, deletion of *VprBP* in zygotes resulted in markedly reduced TET3 protein (Figure 2D) and a concomitant loss of paternal DNA hydroxymethylation (Figure 2E). Deletion of *VprBP* did not affect *Tet3* mRNA level (Figure 2F). These data demonstrate a critical function of VprBP in maintaining the level of Tet3 protein and supporting the activity of Tet enzymes during zygotic development. Zygotic deletion of Tet3 in mice, while abolishing 5mC to 5hmC conversion in the male pronucleus, did not significantly affect early zygotic development (Gu et al., 2011; Wossidlo et al., 2011), suggesting that developmental defects observed in *VprBP*-deficient zygotes involve additional events independent of the defect in paternal chromosome demethylation. Consistent with this notion, we noticed in the *VprBP*-deficient zygotes that pronuclei appeared and DNA more condensed when compared to controls. It is likely that VprBP may have additional substrate(s) that are important for cell cycle progression in zygotes.

CRL4^{VprBP} monoubiquitylates TET proteins

To gain mechanistic insight into VprBP-TET interaction, we first carried out an in vivo ubiquitylation assay in cultured cells. This experiment revealed surprisingly that TET2 is ubiquitylated as a discrete band, which is indicative of monoubiquitylation, rather than a ladder of high-molecular weight conjugates that result from polyubiquitylation (Figure 3A). TET2 ubiquitylation was enhanced by the overexpression of wild-type VprBP, but not either VprBP^{RARA} (Figure S3A) mutant defective in DDB1 binding, VprBP^{N909} mutant lacking the DDB1-binding WD40 domain, or VprBP^{C590} lacking the N-terminal portion involved in TET2 binding (Figure 3A). To directly test the possibility that TET2 is a substrate of CRL4^{VprBP}, we performed an in vivo ubiquitylation assay of TET2 in cells depleted for VprBP, DDB1, or a combination of CUL4A and CUL4B which revealed markedly reduced monoubiquitylation of TET2 after knocking down each individual CRL4 component (Figure 3B). The decrease of TET2 monoubiquitylation by VprBP depletion was restored by ectopic expression of a siRNA-resistant VprBP (Figure S3B), confirming the specificity of VprBP knockdown on TET2 ubiquitylation. CUL4A and CUL4B, although closely related, are distinct in their subcellular localization. Whereas CUL4A resides predominantly in the cytoplasm, CUL4B localizes mostly in the nucleus (Nakagawa and Xiong, 2011). To determine the subcellular location of CRL4^{VprBP}-mediated ubiquitylation of TET2, we knocked down CUL4A and CUL4B separately and examined TET2 ubiquitylation. Monoubiquitylation of TET2 was substantially reduced to a similar level by the depletion of either *CUL4* gene and nearly completely abolished by the combined knock down of both

CUL4 genes (Figure 3C). This result suggests that TET2 can be ubiquitylated in both the cytoplasm and the nucleus and that both CUL4A and CUL4B participate in TET2 monoubiquitylation. Nearly complete elimination of TET2 monoubiquitylation by combined CUL4A and CUL4B knock down also indicated that CRL4^{VprBP} is the major ubiquitin ligase for TET2.

To determine whether TET1 and TET3 are also monoubiquitylated by CRL4A/B^{VprBP}, we knocked down VprBP and examined their ubiquitylation. We found that both ectopically expressed TET1 and TET3 are ubiquitylated as a discrete band which was almost completely abolished by VprBP knockdown (Figure 3D). Conversely, we co-expressed VprBP with either TET1 or TET3 and found a positive correlation between VprBP level and ubiquitylation level of TET1 and TET3 (Figure 3E). Together, these results demonstrate that CRL4A/B^{VprBP} catalyzes monoubiquitylation of all three TET proteins.

We then carried out an in vitro ubiquitylation assay of TET2 and TET3. Incubation of immunopurified TET2 (Figure 3F) or TET3 (Figure S3C) with E1, E2, ubiquitin, ATP and CRL4A^{VprBP} E3 immunocomplex resulted in a clear, single, ubiquitylated species of TET2 and TET3 that were not seen when either E1, E2, or E3 was omitted. In vitro incubation of purified TET2 (Figure 3G) or TET3 (Figure S3D) with a CRL4A^{VprBP} immunocomplex containing mutant VprBP that is deficient in binding to DDB1 (VprBP^{RARA} and VprBP^{N909}) abolished the TET2 monoubiquitylation.

TET proteins are monoubiquitylated by CRL4^{VprBP} E3 ligase at a conserved Lys residue

Unlike degradation-associated polyubiquitylation that does not generally modify a specific lysine residue, monoubiquitylation usually targets a specific lysine. The first attempt to identify the TET monoubiquitylation site by IP-mass spec analyses was not successful (data not shown). We then reasoned that, if CRL4^{VprBP}-mediated TET monoubiquitylation is important for TET function, mutation of the ubiquitylation site in TET2 would cause loss of function in a disease such as AML, in which *TET2* is frequently mutated. In addition to truncations and frameshifts by insertions or deletions, a large number of TET2 missense mutations (>250) have been reported in AML. Intriguingly, we found mutations of only two lysine residues in TET2: K1117 (Gelsi-Boyer et al., 2009; Rocquain et al., 2010) and K1299 (Delhommeau et al., 2009; Jankowska et al., 2009; Kosmider et al., 2009). These mutations were reported to be mutated in two (K1117-to-R) and three (K1299-to-N and K1299-to-E) AML patients, respectively. K1299, but not K1117, is highly conserved among vertebrates as well as TET protein paralogs (Figures 4A, 4B, and Figure S4A). We recreated paralogous AML mutants corresponding to K1299 of human TET2 in mouse Tet2 (K1212N and K1212E), mouse Tet1 (K1537N and K1537E), and mouse Tet3 (K983N and K983E). Both K-to-N and K-to-E mutations of all three TET proteins significantly reduced their respective ubiquitylation, regardless of whether the CD domain (Figure 4C) or full-length TET proteins (Figure 4D) were assayed. We also characterized the K1299R mutant, which replaces the Lys with a similar positively-charged Arg. This replacement also disrupted TET2 ubiquitylation (Figure S4B). A residual ubiquitylated TET was still seen, especially for TET3, when the ubiquitylation site was mutated, but its intensity was not affected by the overexpression of VprBP as the wild-type TET3 (Figure S4C), suggesting that this

conserved lysine residue is the predominant site of VprBP E3 ligase. We conclude that all three TET proteins are primarily monoubiquitylated by CRL4^{VprBP} on a conserved lysine residues paralogous to K1299 in TET2.

To more definitively demonstrate the monoubiquitylated form of TET proteins as a discrete band, we considered the large size of TET proteins (2136, 2002 and 1660 residues for human TET1, TET2 and TET3, respectively) which might causes co-migration of both modified and unmodified forms. To this end, we first co-expressed a shorter CD domain of TET2 (Figure 1B) with VprBP to increase the monoubiquitylated fraction and resolved the lysate by a low percentage (7%) SDS-PAGE. A clearly separated band was seen when TET2 (CD) was singularly expressed. The intensity of this band was 20.2% of that of the unmodified form and was increased to 41.7% after VprBP overexpression (Figure 4E), suggesting that a significant fraction of TET2 can be monoubiquitylated by VprBP. Furthermore, mutations of K1299 to either glutamic acid (KE), asparagine (KN) or arginine (KR) all eliminated this band (Figure 4F).

To examine the ubiquitylation of endogenous TET2 protein, we raised a rabbit polyclonal antibody using a branched human TET2 peptide as an antigen that conjugated the last three amino acid residues of ubiquitin (Arg-Gly-Gly) onto the K1299 residue (see Experimental Procedures for details). After clearing the antibody twice with excess unmodified peptides, we verified the specificity of the anti-UbTET2(K1299) antibody by dot-blot (Figure S4D). The anti-UbTET2(K1299) antibody readily detected a band in cells ectopically expressing wild-type TET2, but no band in cells expressing K1299N mutant TET2 (Figure 4G), validating monoubiquitylation at K1299. We then examined a panel of cell lines for in vivo TET2 ubiquitylation by resolving total cell lysates through a gradient (4-15%) SDS-PAGE to achieve better separation of high molecular proteins. Both the level of total TET2 protein and the intensity of the upper band varied significantly from cell line to cell line (Figure 4H). Immunoblotting of the same lysates with the anti-UbTET2(K1299) antibody detected a single band in U2OS cells that corresponds to the upper band in size, but not in other cell lines that do not express the upper band (lower panel of Figure 4H), confirming the upper band as K1299-monoubiquitylated form of TET2. The upper band of TET2 was expressed at a low level in serum-starved U2OS cells and was stimulated following serum stimulation (Figure 4I). This pattern of the upper band matches perfectly with the band detected by the anti-UbTET2(K1299) antibody (middle panel of Figure 4I). Treatment of cells with PR-619, a non-specific inhibitor of deubiquitylase, increased both the intensity of the upper band and the band detected by the anti-UbTET2(K1299) antibody (Figure 4J). Together, these results demonstrate that TET2 is monoubiquitylated by VprBP-mediated E3 ligase at Lys1299.

VprBP-mediated monoubiquitylation promotes TET binding to DNA *in vitro*

In exploring the functional significance of VprBP-mediated TET monoubiquitylation, we examined several possibilities including the effect of monoubiquitylation on TET's binding to the substrate DNA. Binding of TET proteins to DNA exhibits a preference for DNA containing unmodified cytosine (Ko et al., 2013; Xu et al., 2012). Both wild-type and AML-derived K1299N (KN) and K1299E (KE) mutant TET2 proteins were expressed and immunuopurified from 293T cells and incubated with double-stranded DNA

oligonucleotides containing a single unmethylated or methylated CpG. Gel-shift assay showed that wild-type TET2 bound readily to the unmethylated DNA oligo, as expected. However, both the K1299N and K1299E mutations disrupted the binding (Figure 5A). Mutations targeting the monoubiquitylation site of TET1 and TET3 also disrupted their ability to bind DNA (Figure 5B). Co-expression of VprBP, which increases TET2 monoubiquitylation (Figures 3A and 4E), enhanced TET2 DNA binding (Figure 5C).

We next performed sequential immunopurifications after triple transfection of cells with FLAG-TET2, Myc-VprBP and HA-Ub. We first used the FLAG antibody to purify the total TET2 protein and then the HA antibody to enrich for ubiquitylated TET2. This experiment demonstrated that, when similar amounts of TET2 proteins were incubated with DNA oligonucleotides, TET2 eluted from HA-beads was enriched for monoubiquitylation and bound DNA much stronger than TET2 eluted from FLAG-beads (Figure 5D). The quantification showed that when normalized to total (Flag-tagged) TET2, this sequential IP-enriched ubiquitylated form of TET2 by 4.55 fold which correlates with a 4.5 fold increase of TET2 binding to DNA. Conversely, we performed sequential immunopurification and immunodepletion experiments, first using the FLAG antibody to purify total TET2 proteins and then the HA antibody to deplete ubiquitylated TET2. Depletion substantially removed monoubiquitylated TET2 and, accordingly, decreased DNA binding activity (Figure 5E), supporting the notion that monoubiquitylation promotes TET binding to DNA in vitro.

VprBP-mediated monoubiquitylation promotes TET binding to DNA *in vivo*

To corroborate the in vitro assay, the effect of VprBP-mediated monoubiquitylation on TET2's binding to DNA was determined in cells. ChIP-qPCR assays on multiple, previously identified, TET target sites (Deplus et al., 2013) were performed which showed that wild-type, but not K1299N or K1299E mutant TET2, bound to its target genes (Figure 6A). Co-expression with wild-type, but not RARA or N909 mutant VprBP deficient in DDB1 binding enhanced TET2 DNA binding (Figure 6B). These results support the critical importance of both K1299 and VprBP in promoting TET2 binding to DNA.

The distribution of monoubiquitylated and unmodified TET2 was then determined in cells. It was noted, by direct immunoblotting, that the anti-TET2 antibody predominantly detects one single band in the lysate prepared using a mild NP-40 (0.5%) lysis buffer which does not solubilize chromatin-bound proteins. Two clear bands appeared from lysate prepared using 1% SDS-lysis buffer and boiling which efficiently solubilizes chromatin-associated proteins (Figure 6C). Immunoblotting using the anti-UbTET2(K1299) antibody detected one band in SDS-lysate, but not in NP40-lysate, that corresponds in size to the upper band detected by the TET2 antibody, further supporting the presence of K1299-ubiquitylated TET2 presents predominantly in the NP40-insoluble, nuclear fraction. To directly demonstrate that the monoubiquitylated TET2 binds to chromatin, we separated U2OS whole cell extracts made from a non-ionic detergent (0.1% Triton X-100) lysis buffer into six fractions and determined the distribution of TET2 by direct immunoblotting using anti-TET2 antibody (Figure 6D). We found that upper monoubiquitylated TET2 is present almost exclusively in the chromatin-enriched fraction (P3) and was hardly detectable in the cytosolic (S1, S2 and P2) or soluble nuclear fractions (S3). A very small amount of lower, unmodified TET2 was

also detected in the chromatin fraction. The same assay was repeated using the lysate derived from U2OS cells overexpressing K1299N mutant TET2. It was found that the lower, unmodified band of TET2^{K1299N}, like that wild-type TET2, was not detected in the cytosolic (S1, S2 and P2), but unlike the wild-type TET2, the ubiquitylation-deficient TET2^{K1299N} was not detected in the chromatin-enriched fraction (Figure 6E). Collectively, these results demonstrate that VprBP promotes TET2 protein binding to DNA and that this binding requires the monoubiquitylation at Lys1299.

Oncogenic TET2 mutations disrupt VprBP regulation

To directly test whether monoubiquitylation is critical for TET function *in vivo*, the CD domain and full length of three murine TET proteins that harbor mutations at the ubiquitylation site—Tet1 (K1537N, K1537E); Tet2 (K1212N, K1212E); and Tet3 (K983N, K983E)—were ectopically expressed. TET activity was examined *in vivo* by immunofluorescence using 5hmC antibody. Both wild-type and mutant TET proteins were expressed at similar levels (Figure S5A) and mutation of the monoubiquitylation site did not disrupt binding between the TET proteins and VprBP (Figure S5B). Both K1212E and K1212N (corresponding to K1299E and K1299N in human TET2) mutations targeting the monoubiquitylation site in mouse Tet2 abolished Tet2's activity in catalyzing 5hmC production in cells, whether assayed using full length protein (Figure 7A) or CD domain (Figure S5C). Dot-blot assay using the genomic DNA isolated from transfected cells confirm that both K1212E and K1212N mutants failed to produce 5hmC *in vivo* (Figure S5D), which also applied to both Tet1 and Tet3. Regardless of assaying using the full length and CD domain, mutations targeting the monoubiquitylation site in either Tet1 (Figure S5E) or Tet3 (Figure S5F) also abolished the function of these two Tet enzymes in producing 5hmC in cells under immunofluorescence. Dot-blot assay of genomic DNA further confirmed the loss of activity in producing 5hmC in cells by both mutant Tet1 and Tet3 with disrupted monoubiquitylation site (Figure S5D). These results indicate that VprBP binding to TET proteins *per se* is not sufficient for TET activity, but rather monoubiquitylation is critical for TET activity (see Discussion). Mutation of Lys983 to either Glu (K983E) or Asn (K983N) in both the CD domain and full length Tet3, but not in Tet1 or Tet2, also altered Tet3's almost exclusive nuclear localization to one that is mostly cytoplasmic. Whether monoubiquitylation selectively regulates the subcellular localization of TET3 has not been determined.

TET2 gene is frequently mutated in hematopoietic malignancies. More than half of the mutations result in protein truncation, indicating that loss-of-function is responsible for pathogenesis. In addition, several hundred nonsynonymous point mutations have been reported, but only a few that disrupt the binding of TET2 with either α-KG or Fe^{2+} have been functionally characterized (Ko et al., 2010). Given our finding that two different AML mutations targeting the K1299 monoubiquitylation site of TET2 inactivate its activity *in vivo*, we hypothesized that additional mutation(s) may disrupt both CRL4^{VprBP}-mediated TET2 monoubiquitylation and TET2 activity. A number of AML-derived point mutations surrounding K1299 at the homologous site in mouse Tet2 were created, and their ubiquitylation was determined. Several mutations, in addition to K1299N and K1299E, were found to abolish Tet2 ubiquitylation, including C1298Y, F1300S, and R1302G

(corresponding to C1211Y, F1213S and R1215G in mouse Tet2) (Figure 7B), which has been reported in three, two, and two independent cases of human AML, respectively. Binding analysis revealed that F1213S and R1215G disrupted TET2 binding to VprBP (Figure 7C), providing an explanation of how mutations target these two residues disrupt TET2's monoubiquitylation. However, the C1211Y mutation did not disrupt the monoubiquitylation site nor significantly affect VprBP-TET2 binding, suggesting an additional step after binding of VprBP to TET2 that is important for CRL4^{VprBP}-mediated TET2 monoubiquitylation. Similar to the K1299N and K1299E mutants, ubiquitylation-deficient C1211Y, F1213S and R1215G mutants all lost their activity *in vivo* (Figure 7D). *In vitro* assay using two different substrates, methylated double-stranded DNA (dsDNA) oligonucleotides (Figure S5G) and total genomic DNA (Figure S5H) demonstrate that mutants of TET2 deficient in monoubiquitylation still retain the catalytic activity as determined by the decrease of 5mC and accumulation of 5caC. Together, these results demonstrate that multiple, recurrent AML-derived mutations in TET2 disrupt CRL4^{VprBP}-mediated TET2 monoubiquitylation, while not affecting TET2's catalytic activity, disrupt the VprBP-TET2 binding, the monoubiquitylation site, or another undetermined regulatory step, leading to functional inactivation of TET2 *in vivo* (Figure 7E).

DISCUSSION

VprBP is a critical regulator of TET family dioxygenases

While the biological function and biochemical mechanism of TET enzymes have been extensively investigated, little is known about their regulation at present. We have shown that VprBP is a critical regulator of all three TET enzymes. The importance of VprBP in promoting the function of TET is supported by the genetic evidence that conditional knockout of *Vprbp* in oocytes resulted in a loss of TET3 and abolishment of paternal chromosome 5-hmC. VprBP's importance is also supported by the finding that, in leukemia, multiple recurrent oncogenic mutations in TET2 disrupt VprBP-mediated TET2 activation.

CRL4^{VprBP}-mediated monoubiquitylation promotes TET binding to DNA

We present compelling evidence in this study that VprBP targets the TET proteins for monoubiquitylation by the CRL4^{VprBP} E3 ligase. A lysine residue (K1299 in human TET2), which is invariably conserved among all three TET proteins, is identified as the site of CRL4^{VprBP}-mediated monoubiquitylation. Mutation of this conserved lysine residue abolishes the monoubiquitylation of all three TET proteins. We demonstrated in vivo TET2 monoubiquitylation using the antibody specifically recognizing K1299-ubiquitylated TET2. The abundances of the monoubiquitylated TET2 vary from cell line to cell line, are inhibited by a deubiquitinase inhibitor and are increased when cells are stimulated to enter the cell cycle or when VprBP is overexpressed. These observations indicate that TET2 monoubiquitylation is dynamically regulated in cells.

VprBP-mediated monoubiquitylation plays a critical role in TET activation by promoting their ability to bind DNA, but not catalytic activity of TET enzyme. As binding to DNA is a prerequisite for the function of TET in catalyzing 5mC hydroxylation, our findings provide a molecular basis for the activation of TET dioxygenases by VprBP-mediated

monoubiquitylation. The exact mechanism by which monoubiquitylation promotes TET DNA binding is currently unknown. It is conceivable that conjugation of a ubiquitin could disassociate TET from a factor that blocks TET's binding to DNA, bridge the binding of TET with a factor that recruits TET to DNA, or expose a masked DNA binding domain. Very recently, the crystal structure of a fragment of human TET2 (residues 1129 to 1936) which deleted a large low-complexity region (residues 1481-1843) predicted to be unstructured has been resolved in complex with DNA (Hu et al., 2013). Notably, in this TET2-DNA complex, the K1299 monoubiquitylation site directly contacts DNA. We speculate that monoubiquitylation in TET may directly affect their binding with DNA, for example by stabilizing either the conformation of full-length TET2 containing the unstructured sequence.

Oncogenic mutations in TET2 disrupt VprBP-mediated regulation

The *TET2* gene is frequently mutated in hematopoietic malignancies of both myeloid and lymphoid lineages. The results presented in this study reveal a novel mechanism for oncogenic inactivation of TET2, by disruption of VprBP-mediated monoubiquitylation. As we selectively characterized only a small number of point mutations surrounding the ubiquitylation site, the full spectrum of oncogenic mutations targeting VprBP-mediated TET2 ubiquitylation is unknown and could be underappreciated. *TET* genes are not frequently mutated in solid tumors. Yet, many different types of malignant tissues have been found to contain very low or undetectable levels of 5hmC compared with normal tissues [e.g. ref. (Yang et al., 2013)], implicating additional mechanisms for functionally inactivating TET. In glioma where mutation of a *TET* gene has not been reported, TET enzymes are catalytically inactivated by the D-2-HG oncometabolite produced by mutated IDH1 (Chowdhury et al., 2011; Dang et al., 2009; Xu et al., 2011). The findings reported here present an additional target, CRL4^{VprBP} E3 ligase, for oncogenic inactivation of TET function. It will be important to explore the expression of VprBP and other CRL4 components in different types of tumors.

Experimental Procedures

More detailed descriptions for procedures below and additional procedures are provided in the Supplemental Information.

Mice and oocytes and zygotes analyses

Wild type C57/B6 mice were from the Zhejiang Academy of Medical Science, China. *Vprbp^{flox/flox}* (McCall et al., 2008) and *Zp3-Cre* (Lan et al., 2004) were previously generated. Animal care and experimental procedures were in accordance with the Animal Research Committee guidelines of Zhejiang University. For super-ovulation assay, pubertal mice (21-23 days old) were injected intraperitonally (i.p.) with 5 IU of pregnant mare serum gonadotrophin (PMSG). After 44 hours, the mice were i.p. injected with 5 IU Human chorionic gonadotropin (hCG). After an additional 16 hours, oocyte/cumulus masses were surgically removed from oviducts and the numbers of oocytes were counted. To obtain fertilized eggs (zygotes), female mice were mated. Zygotes were harvested from oviducts at 20 hours after hCG injection and used for confocal microscopy and real-time PCR analyses.

Electrophoretic mobility shift assay

Biotin labeled single-stranded oligonucleotides used for TET-DNA binding assay were synthesized and annealed. 500 ng of immunopurified Flag-TET2 was incubated in a total 20 ul reaction mixture containing 1 ng of biotin labeled oligonucleotide. The resulting protein-DNA complexes were resolved in a 6% DNA retardation gel in $0.5 \times$ TBE buffer, transferred to a nylon membrane and blotted with streptavidin-HRP. The gel-shift assays were performed using the LightShift Chemiluminescent EMSA Kit.

Cell fractionation

4×10^7 U2OS cells were harvested and lysed by Triton X-100. Nuclei were collected in pellet 1 (fraction P1) by low-speed centrifugation (5 min, 1,300g, 4°C). The supernatant (S1) was further clarified by high-speed centrifugation (10 min, 15,000g, 4°C) to remove cell debris and insoluble aggregates (P2). Nuclei were washed once in buffer A, and then lysed. Insoluble chromatin (P3) was collected by centrifugation (5 min, 1,700g, 4°C), washed once in buffer B, and centrifuged again under the same conditions. The resulting six fractions were re-suspended in the Laemmli buffer, boiled for 15min and resolved by SDS-PAGE for western analysis.

In vitro TET2 activity assay

In vitro assay of TET2 catalytic activity was performed using two different substrates, methylated dsDNA oligonucleotides and total genomic DNA. To prepare the TET enzyme, Flag-tagged wild-type and AML-derived full length TET2 mutants were ectopically expressed in HEK293T cells, immunoprecipitated, and eluted by Flag peptide. The reactions were carried out as described in detail in the Supplemental Information, denatured and then neutralized. The reaction mixtures were spotted on nitrocellulose membrane, cross linked and incubated overnight with antibodies recognizing 5mC, 5hmC antibody, 5fC antibody, or 5caC, followed by chemiluminescence.

Supplementary Material

Refer to Web version on PubMed Central for supplementary material.

ACKNOWLEDGEMENTS

REFERENCES

Chowdhury R, Yeoh KK, Tian YM, Hillringhaus L, Bagg EA, Rose NR, Leung IK, Li XS, Woon EC, Yang M, et al. The oncometabolite 2-hydroxyglutarate inhibits histone lysine demethylases. EMBO Rep. 2011; 12:463–469. [PubMed: 21460794]

Costa Y, Ding J, Theunissen TW, Faiola F, Hore TA, Shliaha PV, Fidalgo M, Saunders A, Lawrence M, Dietmann S, et al. NANOG-dependent function of TET1 and TET2 in establishment of pluripotency. Nature. 2013; 495:370–374. [PubMed: 23395962]

Dang L, White DW, Gross S, Bennett BD, Bittinger MA, Driggers EM, Fantin VR, Jang HG, Jin S, Keenan MC, et al. Cancer-associated IDH1 mutations produce 2-hydroxyglutarate. Nature. 2009; 462:739–744. [PubMed: 19935646]

Delhommeau F, Dupont S, Della Valle V, James C, Trannoy S, Masse A, Kosmider O, Le Couedic JP, Robert F, Alberdi A, et al. Mutation in TET2 in myeloid cancers. N Engl J Med. 2009; 360:2289–2301. [PubMed: 19474426]

Deplus R, Delatte B, Schwinn MK, Defrance M, Mendez J, Murphy N, Dawson MA, Volkmar M, Putmans P, Calonne E, et al. TET2 and TET3 regulate GlcNAcylation and H3K4 methylation through OGT and SET1/COMPASS. EMBO J. 2013; 32:645–655. [PubMed: 23353889]

Doege CA, Inoue K, Yamashita T, Rhee DB, Travis S, Fujita R, Guarnieri P, Bhagat G, Vanti WB, Shih A, et al. Early-stage epigenetic modification during somatic cell reprogramming by Parp1 and Tet2. Nature. 2012; 488:652–655. [PubMed: 22902501]

Gelsi-Boyer V, Trouplin V, Adelaide J, Bonansea J, Cervera N, Carbuccia N, Lagarde A, Prebet T, Nezri M, Sainty D, et al. Mutations of polycomb-associated gene ASXL1 in myelodysplastic syndromes and chronic myelomonocytic leukaemia. British J. Haematol. 2009; 145:788–800.

Glickman MH, Ciechanover A. The ubiquitin-proteasome proteolytic pathway: destruction for the sake of construction. Physiol Rev. 2002; 82:373–428. [PubMed: 11917093]

Goll MG, Bestor TH. Eukaryotic cytosine methyltransferases. Annu Rev Biochem. 2005; 74:481–514. [PubMed: 15952895]

Gu TP, Guo F, Yang H, Wu HP, Xu GF, Liu W, Xie ZG, Shi L, He X, Jin SG, et al. The role of Tet3 DNA dioxygenase in epigenetic reprogramming by oocytes. Nature. 2011; 477:606–610. [PubMed: 21892189]

He YF, Li BZ, Li Z, Liu P, Wang Y, Tang Q, Ding J, Jia Y, Chen Z, Li L, et al. Tet-mediated formation of 5-carboxylcytosine and its excision by TDG in mammalian DNA. Science. 2011; 333:1303–1307. [PubMed: 21817016]

Hu L, Li Z, Cheng J, Rao Q, Gong W, Liu M, Shi YG, Zhu J, Wang P, Xu Y. Crystal structure of TET2-DNA complex: insight into TET-mediated 5mC oxidation. Cell. 2013; 155:1545–1555. [PubMed: 24315485]

Ito S, D'Alessio AC, Taranova OV, Hong K, Sowers LC, Zhang Y. Role of Tet proteins in 5mC to 5hmC conversion, ES-cell self-renewal and inner cell mass specification. Nature. 2010; 466:1129–1133. [PubMed: 20639862]

Ito S, Shen L, Dai Q, Wu SC, Collins LB, Swenberg JA, He C, Zhang Y. Tet proteins can convert 5-methylcytosine to 5-formylcytosine and 5-carboxylcytosine. Science. 2011; 333:1300–1303. [PubMed: 21778364]

Jackson S, Xiong Y. CRL4s: the CUL4-RING E3 ubiquitin ligases. Trends Biochem Sci. 2009; 34:562–570. [PubMed: 19818632]

Jankowska AM, Szpurka H, Tiu RV, Makishima H, Afable M, Huh J, O'Keefe CL, Ganetzky R, McDevitt MA, Maciejewski JP. Loss of heterozygosity 4q24 and TET2 mutations associated with myelodysplastic/myeloproliferative neoplasms. Blood. 2009; 113:6403–6410. [PubMed: 19372255]

Ko M, Huang Y, Jankowska AM, Pape UJ, Tahiliani M, Bandukwala HS, An J, Lamperti ED, Koh KP, Ganetzky R, et al. Impaired hydroxylation of 5-methylcytosine in myeloid cancers with mutant TET2. Nature. 2010; 468:839–843. [PubMed: 21057493]

Kosmider O, Gelsi-Boyer V, Cheok M, Grabar S, Della-Valle V, Picard F, Viguie F, Quesnel B, Beyne-Rauzy O, Solary E, et al. TET2 mutation is an independent favorable prognostic factor in myelodysplastic syndromes (MDSs). Blood. 2009; 114:3285–3291. [PubMed: 19666869]

Lewandoski M, Wassarman KM, Martin GR. Zp3-cre, a transgenic mouse line for the activation or inactivation of loxP-flanked target genes specifically in the female germ line. Curr Biol. 1997; 7:148–151. [PubMed: 9016703]

Li E. Chromatin modification and epigenetic reprogramming in mammalian development. Nat Rev Genet. 2002; 3:662–673. [PubMed: 12209141]

McCall CM, Miliani de Marval PL, Chastain PD 2nd, Jackson SC, He YJ, Kotake Y, Cook JG, Xiong Y. Human immunodeficiency virus type 1 Vpr-binding protein VprBP, a WD40 protein associated

with the DDB1-CUL4 E3 ubiquitin ligase, is essential for DNA replication and embryonic development. Mol Cell Biol. 2008; 28:5621–5633. [PubMed: 18606781]

Mellen M, Ayata P, Dewell S, Kriaucionis S, Heintz N. MeCP2 binds to 5hmC enriched within active genes and accessible chromatin in the nervous system. Cell. 2012; 151:1417–1430. [PubMed: 23260135]

Nakagawa T, Mondal K, Swanson PC. VprBP (DCAF1): A promiscuous substrate recognition subunit that incorporates into both RING-family CRL4 and HECT-family EDD/UBR5 E3 ubiquitin ligases. BMC Mol Biol. 2013; 14:22. [PubMed: 24028781]

Nakagawa T, Xiong Y. X-linked mental retardation gene CUL4B targets ubiquitylation of H3K4 methyltransferase component WDR5 and regulates neuronal gene expression. Mol Cell. 2011; 43:381–391. [PubMed: 21816345]

Piccolo FM, Bagci H, Brown KE, Landeira D, Soza-Ried J, Feytout A, Mooijman D, Hajkova P, Leitch HG, Tada T, et al. Different Roles for Tet1 and Tet2 Proteins in Reprogramming-Mediated Erasure of Imprints Induced by EGC Fusion. Mol Cell. 2013; 49:1023–1021. 1033. [PubMed: 23453809]

Quivoron C, Couronne L, Della Valle V, Lopez CK, Plo I, Wagner-Ballon O, Do Cruzeiro M, Delhommeau F, Arnulf B, Stern MH, et al. TET2 inactivation results in pleiotropic hematopoietic abnormalities in mouse and is a recurrent event during human lymphomagenesis. Cancer cell. 2011; 20:25–38. [PubMed: 21723201]

Rocquain J, Carbuccia N, Trouplin V, Raynaud S, Murati A, Nezri M, Tadrist Z, Olschwang S, Vey N, Birnbaum D, et al. Combined mutations of ASXL1, CBL, FLT3, IDH1, IDH2, JAK2, KRAS, NPM1, NRAS, RUNX1, TET2 and WT1 genes in myelodysplastic syndromes and acute myeloid leukemias. BMC cancer. 2010; 10:401. [PubMed: 20678218]

Tahiliani M, Koh KP, Shen Y, Pastor WA, Bandukwala H, Brudno Y, Agarwal S, Iyer LM, Liu DR, Aravind L, Rao A. Conversion of 5-methylcytosine to 5-hydroxymethylcytosine in mammalian DNA by MLL partner TET1. Science. 2009; 324:930–935. [PubMed: 19372391]

Tefferi A, Pardanani A, Lim KH, Abdel-Wahab O, Lasho TL, Patel J, Gangat N, Finke CM, Schwager S, Mullally A, et al. TET2 mutations and their clinical correlates in polycythemia vera, essential thrombocythemia and myelofibrosis. Leukemia. 2009; 23:905–911. [PubMed: 19262601]

Wossidlo M, Nakamura T, Lepikhov K, Marques CJ, Zakhartchenko V, Boiani M, Arand J, Nakano T, Reik W, Walter J. 5-Hydroxymethylcytosine in the mammalian zygote is linked with epigenetic reprogramming. Nat Commun. 2011; 2:241. [PubMed: 21407207]

Wu H, Zhang Y. Reversing DNA Methylation: Mechanisms, Genomics, and Biological Functions. Cell. 2014; 156:45–68. [PubMed: 24439369]

Xu W, Yang H, Liu Y, Yang Y, Wang P, Kim SH, Ito S, Yang C, Xiao MT, Liu LX, et al. Oncometabolite 2-hydroxyglutarate is a competitive inhibitor of alpha-ketoglutarate-dependent dioxygenases. Cancer Cell. 2011; 19:17–30. [PubMed: 21251613]

Xu Y, Xu C, Kato A, Tempel W, Abreu JG, Bian C, Hu Y, Hu D, Zhao B, Cerovina T, et al. Tet3 CXXC domain and dioxygenase activity cooperatively regulate key genes for Xenopus eye and neural development. Cell. 2012; 151:1200–1213. [PubMed: 23217707]

Yamaguchi S, Hong K, Liu R, Shen L, Inoue A, Diep D, Zhang K, Zhang Y. Tet1 controls meiosis by regulating meiotic gene expression. Nature. 2012; 492:443–447. [PubMed: 23151479]

Yang H, Liu Y, Bai F, Zhang JY, Ma SH, Liu J, Xu ZD, Zhu HG, Ling ZQ, Ye D, et al. Tumor development is associated with decrease of TET gene expression and 5-methylcytosine hydroxylation. Oncogene. 2013; 32:663–669. [PubMed: 22391558]

Yildirim O, Li R, Hung JH, Chen PB, Dong X, Ee LS, Weng Z, Rando OJ, Fazzio TG. Mbd3/NURD complex regulates expression of 5-hydroxymethylcytosine marked genes in embryonic stem cells. Cell. 2011; 147:1498–1510. [PubMed: 22196727]

Yu M, Hon GC, Szulwach KE, Song CX, Zhang L, Kim A, Li X, Dai Q, Shen Y, Park B, et al. Base-resolution analysis of 5-hydroxymethylcytosine in the mammalian genome. Cell. 2012; 149:1368–1380. [PubMed: 22608086]
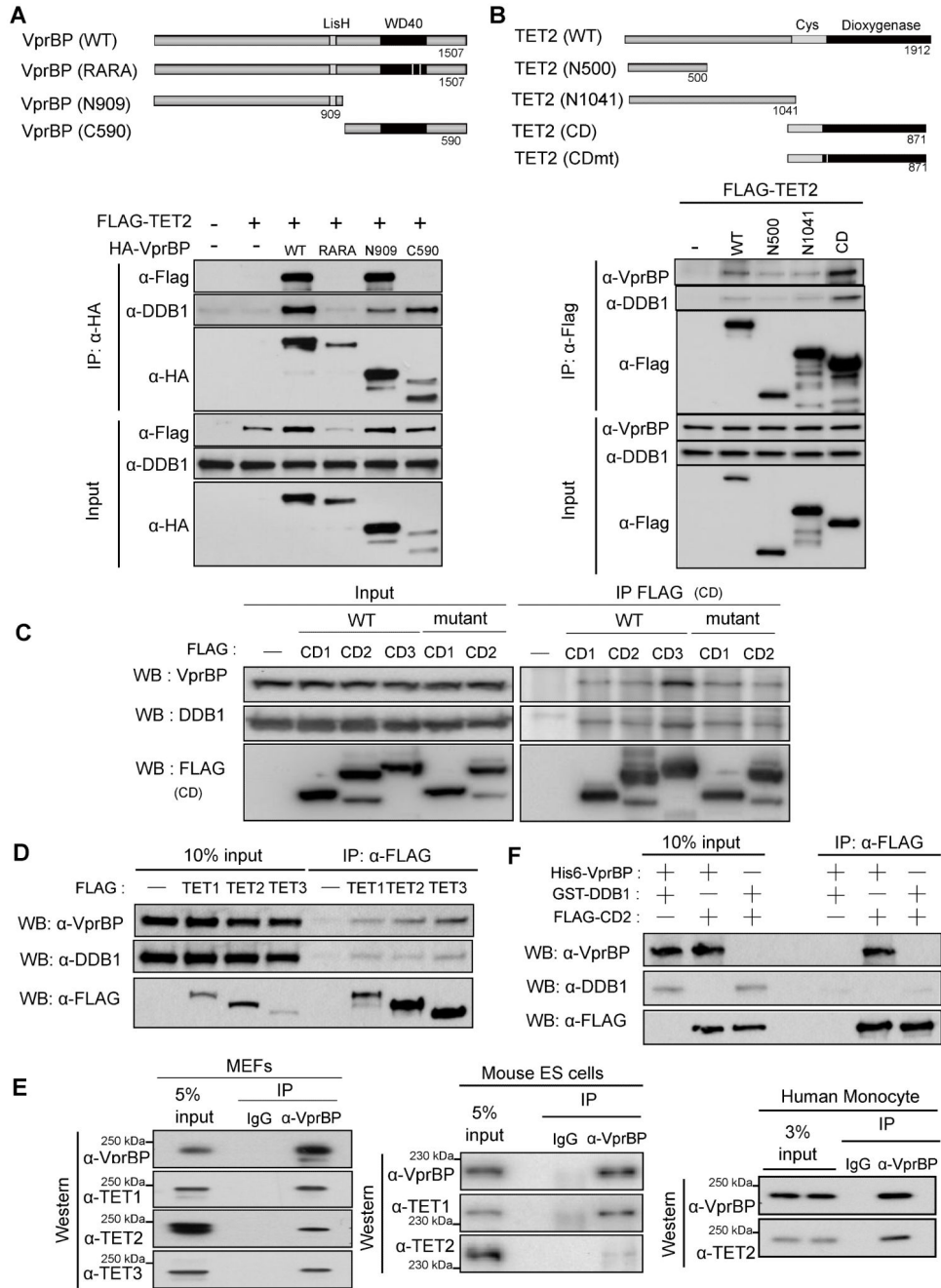
Figure 1. VprBP binds to TET family proteins

(**A**) Top, Domain structure of human VprBP. Bottom, 293T cells were transiently transfected with expression vectors for FLAG-TET2 and a series of HA-VprBP fragments. Cell lysates were subjected to IP with an HA antibody, followed by Western blot (WB). (**B**) Top, Domain structure of mouse TET2. Bottom, 293T cells were transiently transfected with expression vectors for a series of FLAG-TET2 fragments. Cell lysates were subjected to IP with FLAG antibody, followed by WB. CD: cysteine-rich, dioxygenase domain.

(**C**) FLAG-tagged mouse TET CD domains were immunoprecipitated from 293T cells and their associated proteins were detected by WB. CD1, CD2 and CD3 refer to the CD domain of mouse TET1 (residue 1400 to 2039, NP_001240786.1), TET2 (residue 1042 to 1912, NP_081660.1) and TET3 (residue 697 to 1668, NP_898961.2), respectively. CM: catalytic mutant (H1620Y/D1622A for mouse TET1, H1295Y/D1297A for mouse TET2).

(**D**) FLAG-TET proteins were immunoprecipitated from 293T cells and their associated proteins were detected by WB.

(**E**) Endogenous VprBP was immunoprecipitated from MEF, mouse ES cells and human monocytes and its association with TET proteins was determined by WB.

(**F**) Recombinant FLAG-TET2-CD was incubated with recombinant His_6-VprBP or GST-DDB1. Binding was monitored by WB.

See also Figure S1 and Table S1, S2.
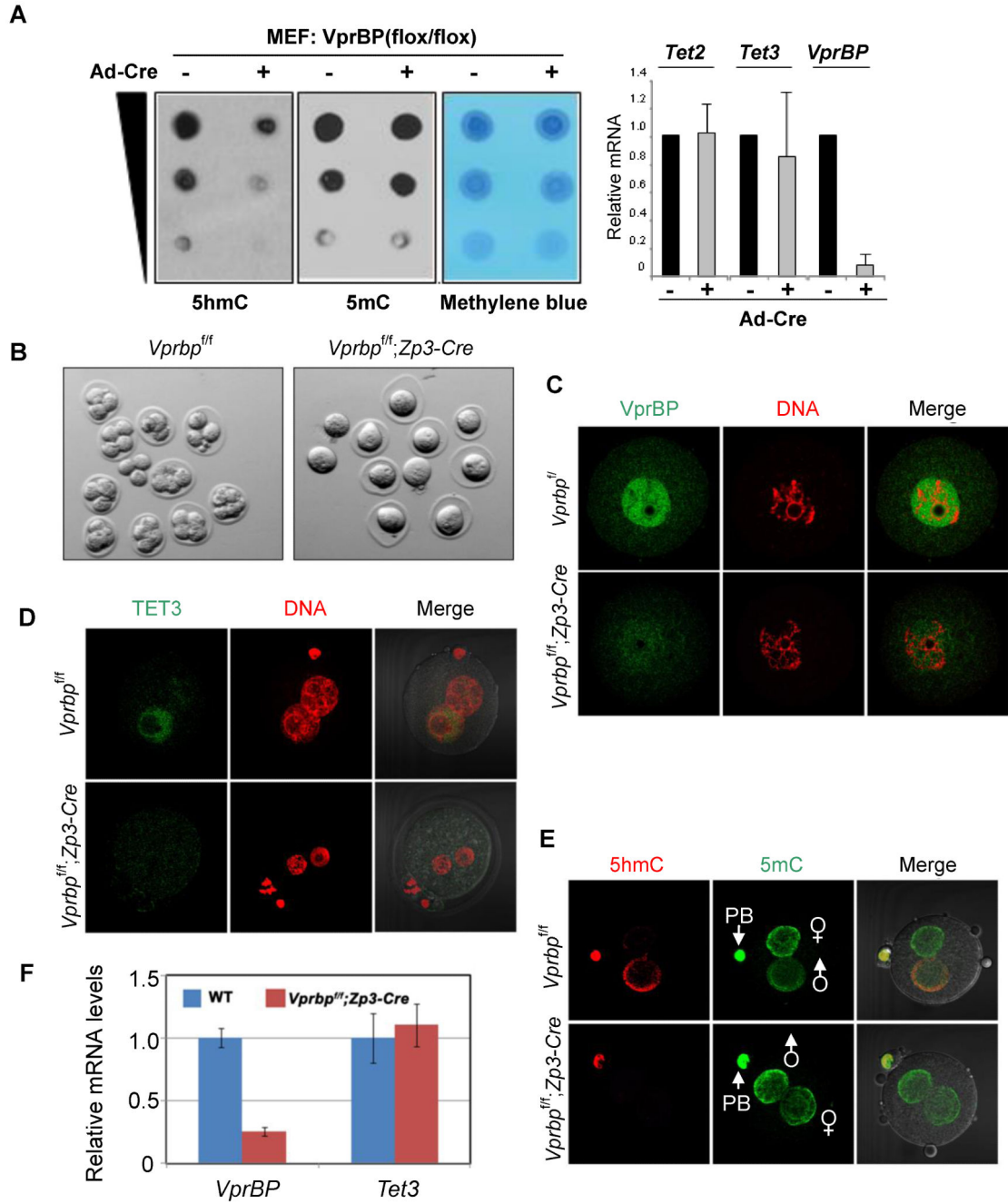
Figure 2. VprBP is essential for TET activity

(**A**) *VprBP^{f/f}* MEFs were infected with adenovirus expressing Cre. mRNA level was analyzed by quantitative RT-PCR and 5mC and 5hmC level was analyzed by dot blot. (**B**) Female *Vprbp*^{f/f} and *Vprbp*^{f/f};*Zp3-Cre* mice were superovulated with PMSG and hCG before mating to wild-type males. Successful mating was confirmed by the presence of vaginal plugs. 48 hours after hCG, embryos were obtained from the oviducts and examined microscopically.

(**C**) The expression of VprBP in *VprBP^{f/f}* or *VprBP^{f/f};Zp3-Cre* oocytes from the germinal vesicle (GV) stage was examined by immunofluorescence. (**D**, **E**) The expression of Tet3 (B), 5mC and 5hmC (C) in *VprBP^{f/f}* or *VprBP^{f/f};Zp3-Cre* oocyte-derived zygotes were examined by immunofluorescence. (**F**) The expression of *VprBP* and *Tet3* mRNA in *VprBP^{f/f}* or *VprBP^{f/f};Zp3-Cre* oocytes from germinal vesicle (GV) stage was determined by quantitative RT-PCR analysis.

See also Figure S2 and Table S2, S3.
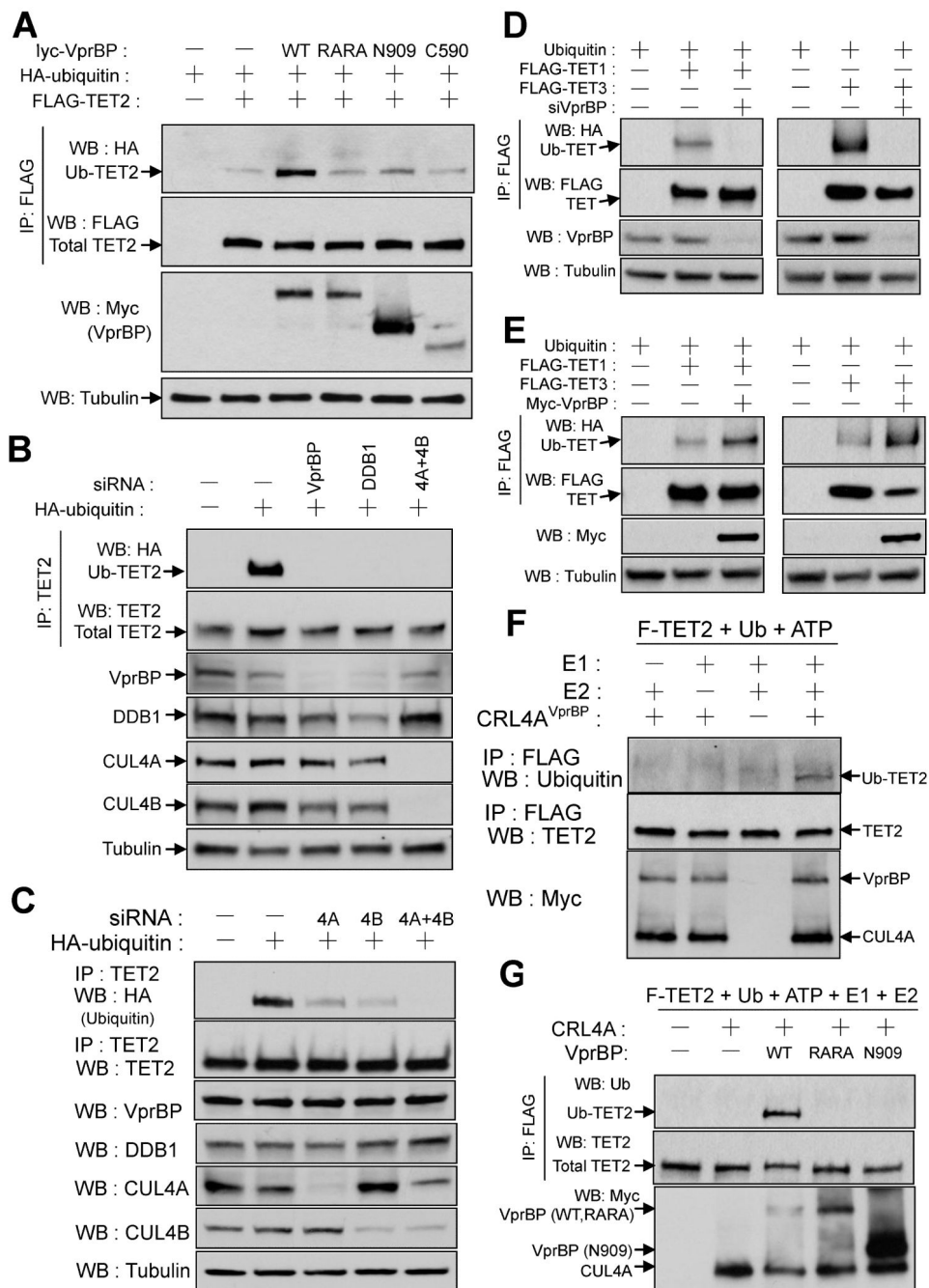
Figure 3. CRL4^VprBP monoubiquitylates TET proteins

(**A**) 293T cells transfected with plasmids of Myc-VprBP, FLAG-TET2, and HA-ubiquitin were lysed and subjected to IP with an antibody to FLAG under denaturing conditions (0.1% SDS). The resulting precipitates were blotted with the indicated antibodies.

(**B**) 293T cells were transfected with plasmids of HA-ubiquitin along with siRNA for VprBP, DDB1, or CUL4 and subsequently lysed and subjected to IP with an antibody to TET2 under denaturing conditions. Precipitates were immunoblotted.

(**C**) 293T cells transfected with a plasmid of HA-ubiquitin along with siRNA for CUL4A, CUL4B or CUL4A and CUL4B were lysed and subjected to IP with an antibody to TET2 under denaturing conditions. Precipitates were blotted.

(**D**) In vivo ubiquitylations of ectopically expressed TET1 and TET3 proteins were determined in cells transfected with siRNA targeting VprBP.

(**E**) In vivo ubiquitylations of ectopically expressed TET1 and TET3 proteins were determined in cells with or without co-expression of VprBP.

(**F**) Recombinant FLAG-TET2 was incubated with different combinations of E1, E2, and CRL4A^{VprBP} (E3) along with ATP and ubiquitin, followed by IP with a FLAG antibody. Ubiquitylated TET2 was examined by WB with anti-ubiquitin.

(**G**) Recombinant FLAG-TET2 was incubated with ubiquitin, E1, E2, CRL4A along with different combinations of VprBP mutants, followed by IP with a FLAG antibody.

See also Figure S3, Table S2.

A

H.sapiens	1290	SWSMYYNGC**K**FARSKIPRKF
M. musculus	1203	SWSMYYNGC**K**FARSKKPRKF
G. gallus	1263	SWSMYYNGC**K**FARSKIPRKF
A. carolinensis	947	SWSMYYNGC**K**FARSKIPRKF
X. laevis	1138	SWSMFYNGC**K**YARSKTPRKF
D. rerio	1261	SWSMFYNGC**K**YARSKVPRKF

B

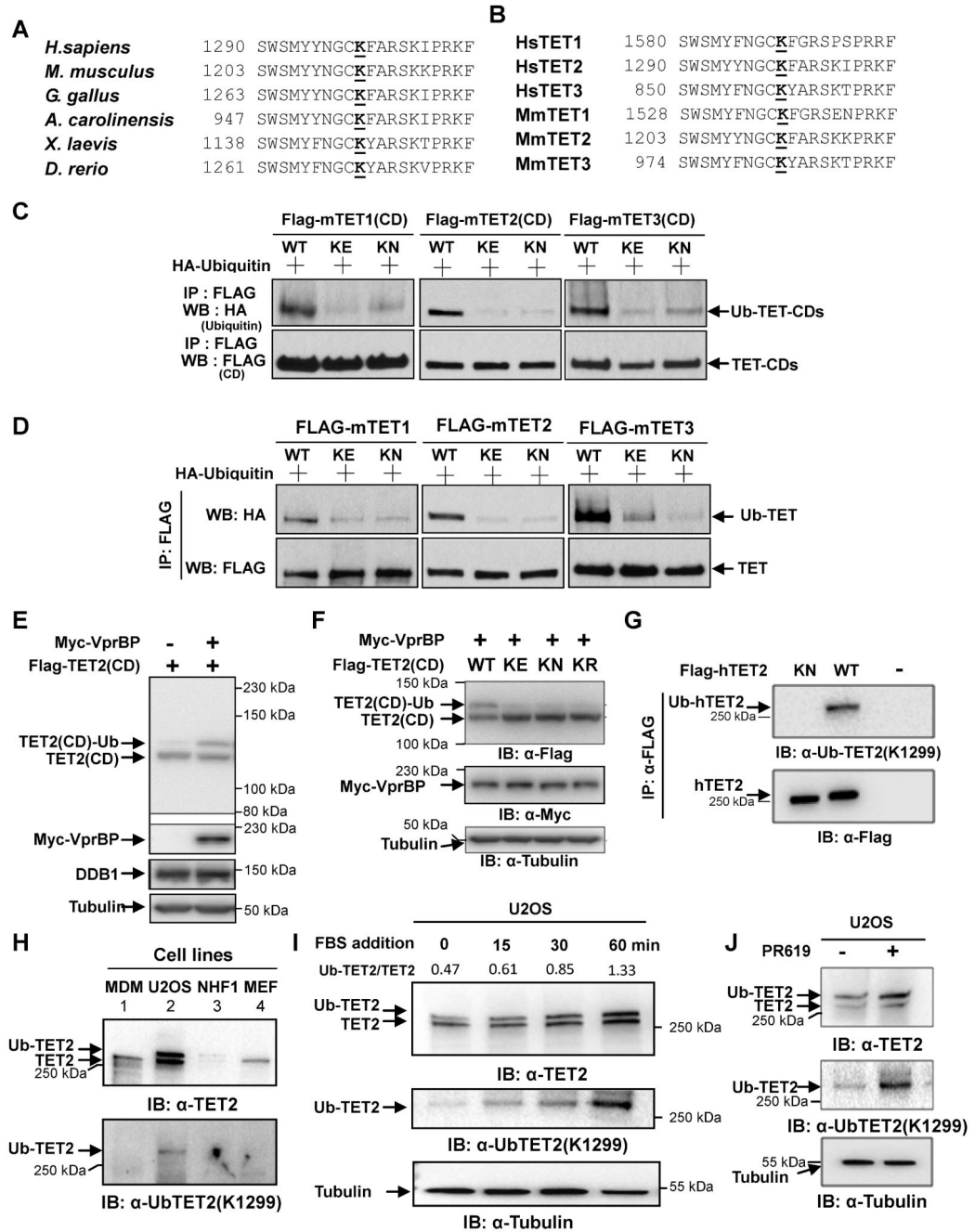|		
HsTET1	1580	SWSMFYNGC**K**FGRSPSPRRF
HsTET2	1290	SWSMYYNGC**K**FARSKIPRKF
HsTET3	850	SWSMFYNGC**K**YARSKTPRKF
MmTET1	1528	SWSMFYNGC**K**FGRSENPRKF
MmTET2	1203	SWSMYYNGC**K**FARSKKPRKF
MmTET3	974	SWSMFYNGC**K**YARSKTPRKF

C

Flag-mTET1(CD)   Flag-mTET2(CD)   Flag-mTET3(CD)
WT KE KN   WT KE KN   WT KE KN
HA-Ubiquitin + + +   + + +   + + +
IP : FLAG WB : HA (Ubiquitin) ← Ub-TET-CDs
IP : FLAG WB : FLAG (CD) ← TET-CDs

D

FLAG-mTET1   FLAG-mTET2   FLAG-mTET3
WT KE KN   WT KE KN   WT KE KN
HA-Ubiquitin + + +   + + +   + + +
IP: FLAG WB: HA ← Ub-TET
WB: FLAG ← TET

E

Myc-VprBP − +
Flag-TET2(CD) + +
TET2(CD)-Ub → 230 kDa / 150 kDa
TET2(CD) →
100 kDa / 80 kDa
Myc-VprBP → 230 kDa
DDB1 → 150 kDa
Tubulin → 50 kDa

F

Myc-VprBP + + + +
Flag-TET2(CD) WT KE KN KR
150 kDa
TET2(CD)-Ub →
TET2(CD) →
100 kDa
IB: α-Flag
230 kDa
Myc-VprBP →
IB: α-Myc
50 kDa
Tubulin →
IB: α-Tubulin

G

Flag-hTET2 KN WT −
Ub-hTET2 → 250 kDa
IB: α-Ub-TET2(K1299)
IP: α-FLAG
hTET2 → 250 kDa
IB: α-Flag

H

Cell lines
MDM U2OS NHF1 MEF
1 2 3 4
Ub-TET2 →
TET2 →
250 kDa
IB: α-TET2
Ub-TET2 → 250 kDa
IB: α-UbTET2(K1299)

I

U2OS
FBS addition 0 15 30 60 min
Ub-TET2/TET2 0.47 0.61 0.85 1.33
Ub-TET2 →
TET2 →
250 kDa
IB: α-TET2
Ub-TET2 → 250 kDa
IB: α-UbTET2(K1299)
Tubulin → 55 kDa
IB: α-Tubulin

J

U2OS
PR619 − +
Ub-TET2 →
TET2 →
250 kDa
IB: α-TET2
Ub-TET2 → 250 kDa
IB: α-UbTET2(K1299)
Tubulin → 55 kDa
IB: α-Tubulin

Figure 4. CRL4^{VprBP} ubiquitylates TET proteins on a conserved Lys residue

(**A**) Sequence alignment of TET2 surrounding K1299 from various vertebrate species, including human (*H. sapiens*, NCBI reference number: NP_001120680.1), mouse (*M. musculus*, NP_001035490), chicken (*G. gallus*, NP_001264723), lizard (*A. carolinensis*, XP_003226445.1), frog (*X. laevis*, ADU77105), and zebrafish (*D. rerio*, XP_005168673). (**B**) Sequence alignment of the human and mouse TET proteins surrounding human TET2-K1299, including human TET1 (NP_085128.2), TET2 (NP_001120680.1), TET3

(NP_659430.1), mouse TET1 (NP_081660), TET2 (NP_001035490.2) and TET3 (ADR57138.1).

(**C, D**). Ubiquitylation of the CD domain (C) and full length (D) mouse TET proteins were determined in 293T cells transfected with plasmids expressing HA-ubiquitin, WT TET2, AML-derived K1299 mutant TET2, or the corresponding AML-derived TET1 and TET3 mutants. Cells were lysed and subjected to IP with a FLAG antibody under denaturing conditions. Precipitates were blotted.

(**E**) 293T cells were transfected with a plasmid expressing the FLAG-tagged human TET2 CD domain and Myc-VprBP as indicated. Total protein lysates were separated on a 7% SDS-PAGE and blotted.

(**F**) 293T cells were co-transfected with plasmids expressing Myc-VprBP and FLAG-tagged WT or mutant TET2 CD domains as indicated. Total protein lysates were separated on a 7% SDS-PAGE and blotted. KE: K1299E; KN: K1299N, KR: K1299R.

(**G**) 293T cells were transfected with plasmid expressing indicated WT or ubiquitylation site mutant (KN) human TET2 protein. Cells were lysed in SDS (1%) buffer, diluted for 10 fold and subjected to IP with Flag beads under denaturing conditions. Precipitates were blotted with Flag and UbTET2 (K1299) antibodies.

(**H**) Total protein extracts were prepared from indicated cell lines using a SDS (1%) lysis buffer and revolved through a gradient (4-15%) SDS-PAGE, and blotted with either TET2 and UbTET2(K1299) antibody.

(**I**) U2OS cells were serum deprived for 24h followed by FBS stimulation according to the indicated time course. The cells were then lysed with 1% SDS buffer and blotted with TET2 and UbTET2(K1299) antibody. The relative amount of monoubiquitylated TET2 was determined by normalization to unmodified TET2.

(**J**) U2OS cells were treated with 8 μM PR619 for 24h, lysed with 1%SDS buffer, and blotted with TET2 and UbTET2(K1299) antibody.
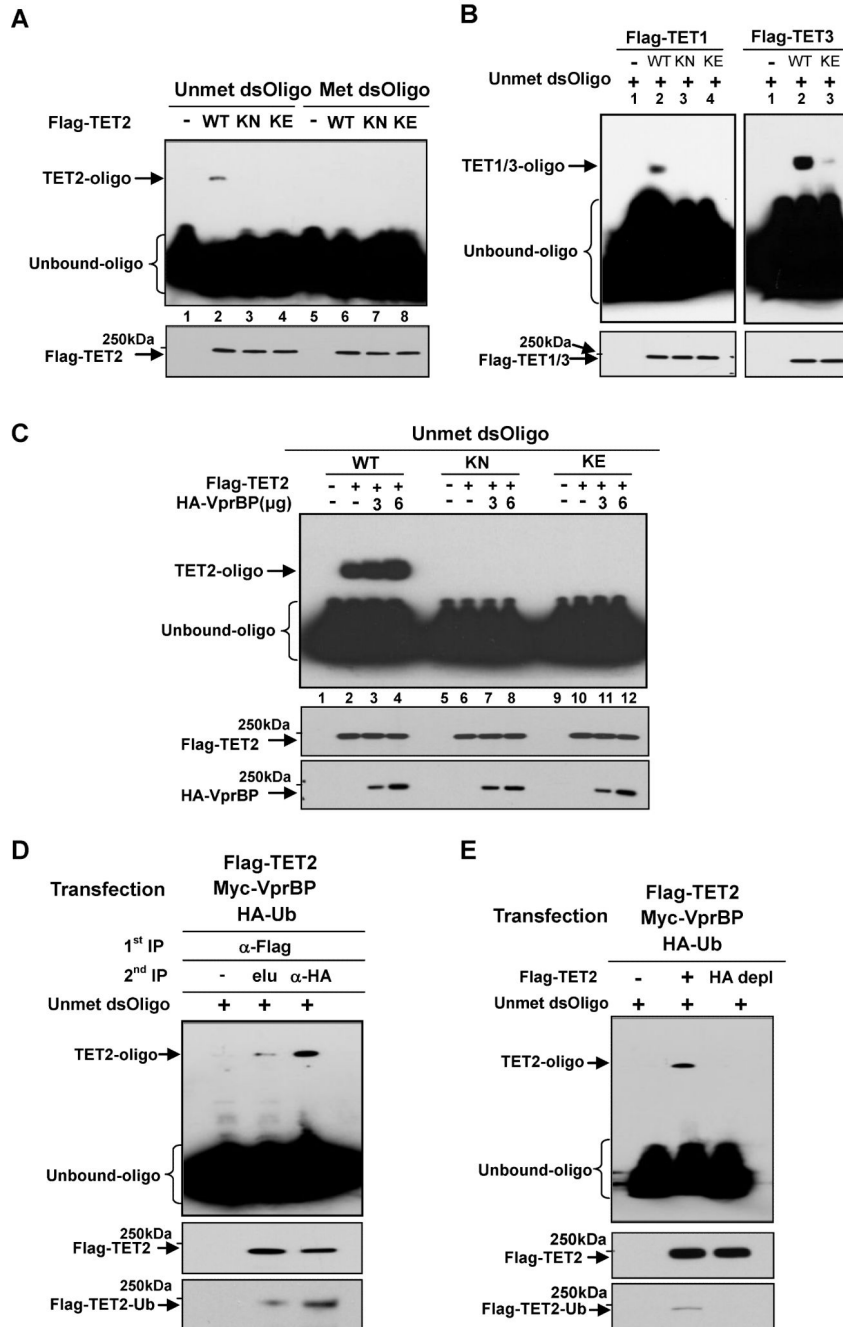
See also Figure S4, Table S2.

Figure 5. VprBP-mediated monoubiquitylation promotes TET binding to DNA *in vitro*

(**A**) 293T cells were transfected with a plasmid expressing FLAG-tagged WT or AML-derived mutant TET2 as indicated. TET2 proteins were immunopurified and incubated with double-stranded DNA oligonucleotides containing a single unmethylated or methylated CpG. Protein-DNA binding was determined by gel-shift assay. Protein levels were analyzed by WB.

(**B**) 293T cells were transfected with a plasmid expressing FLAG-tagged WT or mutant TET1 or TET3 as indicated. Proteins were immunopurified from 293T cells and incubated

with double-stranded DNA oligonucleotides containing a single unmethylated CpG. Protein-DNA binding was determined by gel-shift assay. Protein levels were analyzed by WB.

(**C**) 293T cells were transfected either alone with plasmids expressing FLAG-tagged WT or mutant TET2, or co-transfected with HA-VprBP as indicated. Proteins were immunopurified from 293T cells and incubated with DNA oligonucleotides containing a single unmethylated CpG. Protein-DNA binding was determined by gel-shift assay. Protein levels were analyzed by WB.

(**D**) 293T cells were triply transfected with FLAG-TET2, Myc-VprBP and HA-Ub. Sequential immunopurification was performed: first using the antibody to FLAG to purify TET2 protein and then the antibody to HA to enrich ubiquitylated TET2. DNA binding activity of proteins eluted from FLAG beads or HA beads was determined by gel-shift assay. Protein and ubiquitylation levels were analyzed by WB.

(**E**) 293T cells were triply transfected with FLAG-TET2, Myc-VprBP and HA-Ub. Immunopurification and immunodepletion was performed: first using the antibody to FLAG to purify TET2 protein and then the antibody to HA to deplete ubiquitylated TET2. DNA binding activity of proteins before or after HA depletion was determined by gel-shift assay. Protein and ubiquitylation levels were analyzed by WB.
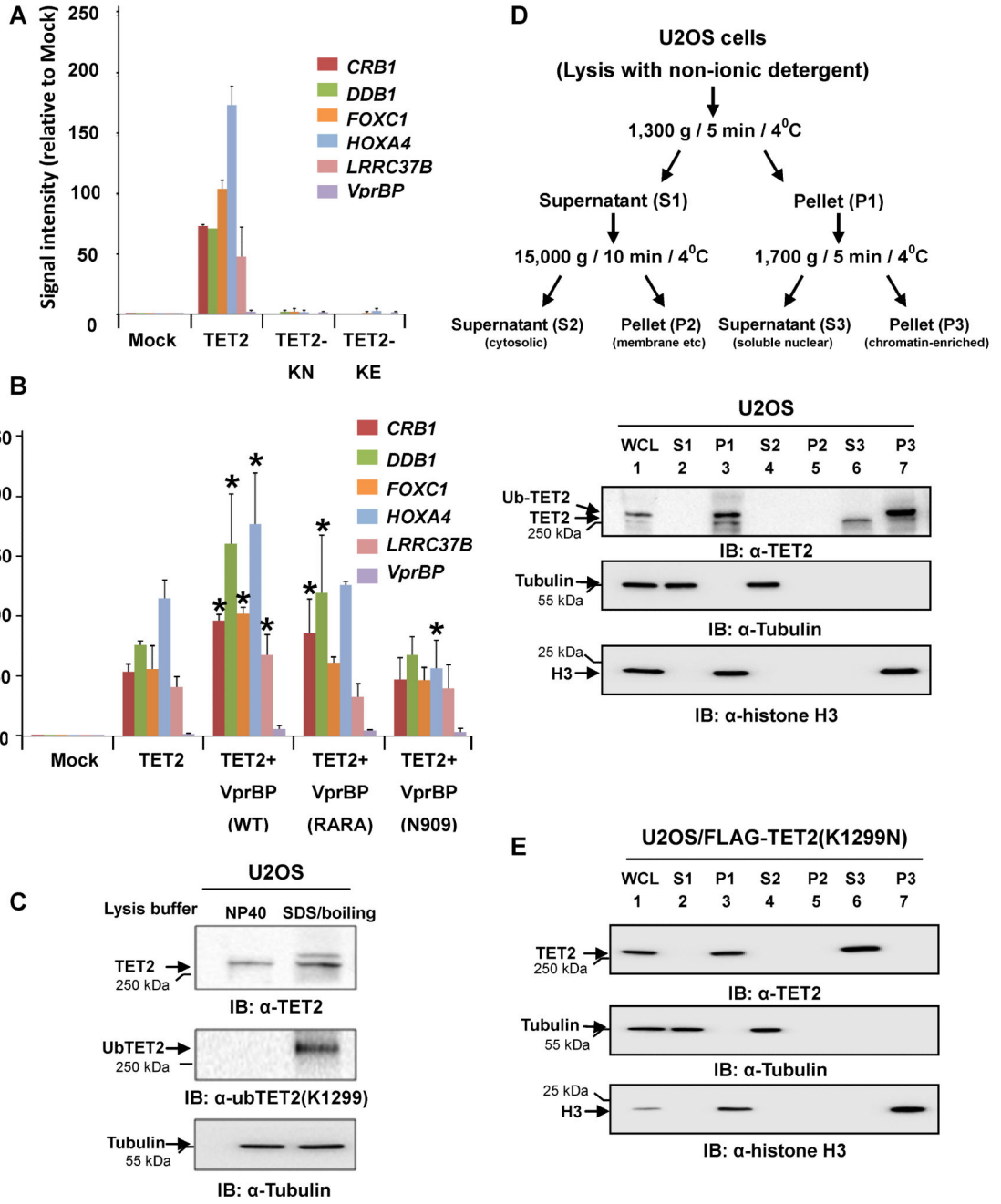
See also Table S2.

Figure 6. VprBP-mediated monoubiquitylation promotes TET binding to DNA *in vivo*
(**A**) 293T cells were transfected with plasmid DNA encoding FLAG-tagged WT or lysine mutants of TET2. DNA/protein complexes were cross-linked and subjected to ChIP analysis with a FLAG antibody. Immunoprecipitates were analyzed by quantitative PCR (qPCR) with primers for the indicated TET2 target gene promoters. The signal intensity on the y axes represents the fold enrichment of DNA amplified by qPCR from cells expressing TET2 compared with that from mock cells transfected with empty vector. See Table S4 for primer sequences.

(**B**) 293T cells were transfected with plasmid DNAs expressing FLAG-tagged TET2 and WT or mutant VprBP proteins as indicated. ChIP-qPCR analyses were performed as in Figure 6A. The signal intensity on the y axes represents the fold enrichment of DNA amplified by qPCR from cells expressing TET2 compared with that from mock cells transfected with empty vector. See Table S4 for primer sequences.

(**C**) U2OS cells were lysed with 0.5% NP40 or 1% SDS buffer, followed by WB with TET2 and UbTET2(K1299) antibody, respectively.

(**D**) U2OS cells were lysed in a non-ionic (0.1% Triton X-100) lysis buffer and lysates were separated into six fractions, followed by WB.

(**E**) U2OS cells were transfected with a plasmid expressing K1299N mutant TET2 and then lysed, fractionated and blotted as Figure 6D.
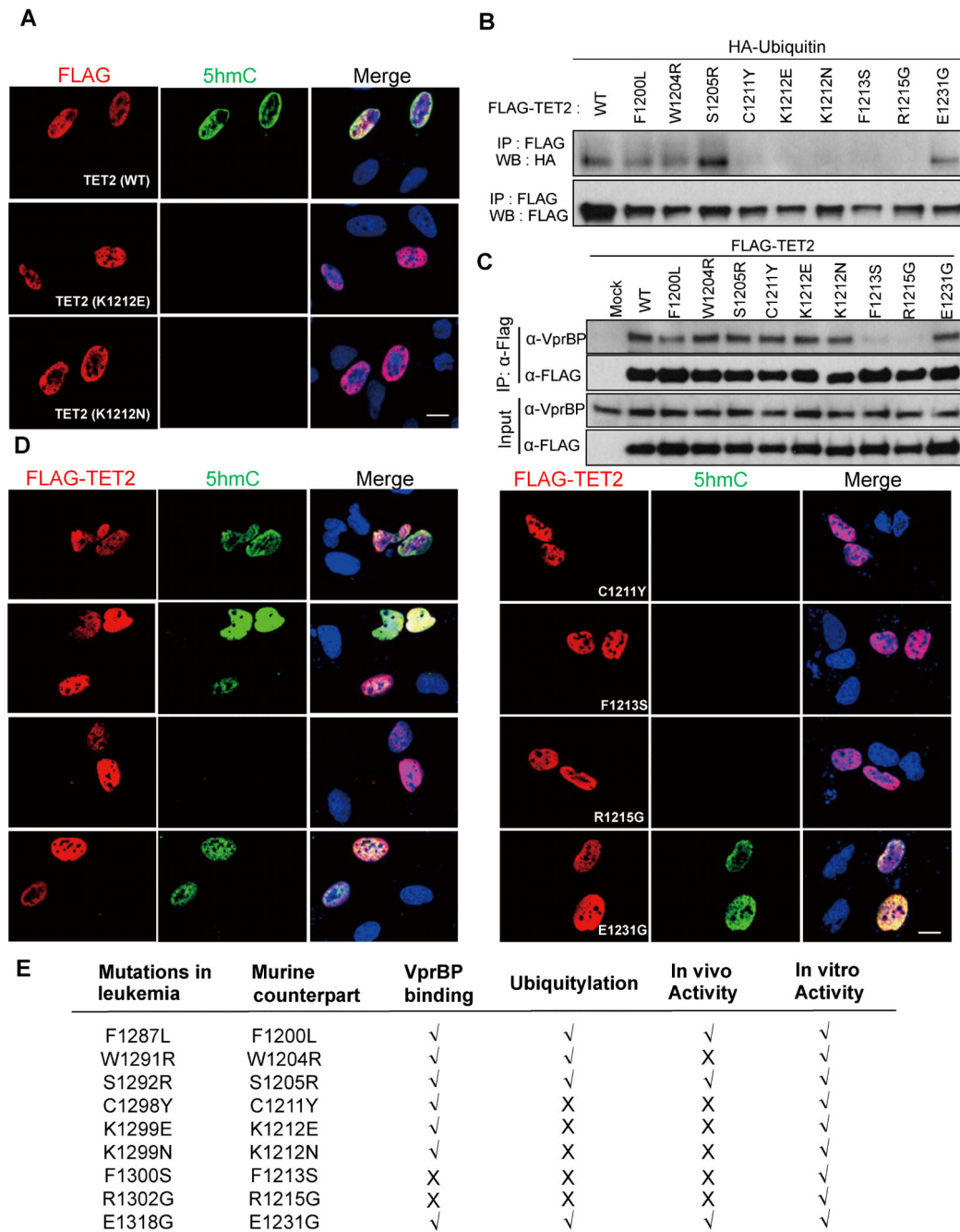
See also Table S2, S4.

A

FLAG   5hmC   Merge

TET2 (WT)

TET2 (K1212E)

TET2 (K1212N)

B

HA-Ubiquitin

FLAG-TET2 : WT F1200L W1204R S1205R C1211Y K1212E K1212N F1213S R1215G E1231G

IP : FLAG
WB : HA

IP : FLAG
WB : FLAG

C

FLAG-TET2

Mock WT F1200L W1204R S1205R C1211Y K1212E K1212N F1213S R1215G E1231G

IP: α-Flag
α-VprBP
α-FLAG

Input
α-VprBP
α-FLAG

D

FLAG-TET2   5hmC   Merge

FLAG-TET2   5hmC   Merge

C1211Y

F1213S

R1215G

E1231G

E

Mutations in leukemia	Murine counterpart	VprBP binding	Ubiquitylation	In vivo Activity	In vitro Activity
F1287L	F1200L	√	√	√	√
W1291R	W1204R	√	√	X	√
S1292R	S1205R	√	√	√	√
C1298Y	C1211Y	√	X	X	√
K1299E	K1212E	√	X	X	√
K1299N	K1212N	√	X	X	√
F1300S	F1213S	X	X	X	√
R1302G	R1215G	X	X	X	√
E1318G	E1231G	√	√	√	√

Figure 7. Multiple recurrent leukemia-derived mutations in TET2 disrupt VprBP-mediated TET2 monoubiquitylation

(**A**) U2OS cells were transiently transfected with an expression vector for FLAG-TET2 or the TET2 lysine mutant, and the cells were fixed and immunostained with anti-FLAG (red) and anti-5hmC (green) antibodies. The nucleus was visualized by DAPI. Scale bar, 10 μm.

(**B**) The in vivo ubiquitylation level of TET2 leukemia mutants was examined by IP followed by WB.

(**C**) Binding of TET2 leukemia mutants to VprBP was examined by IP followed by WB.

(**D**) Activity of TET2 leukemia mutants was examined by immunofluorescence. See Figure S5D for the dot-blot assay and also Figure S5E and S5F for the similar assays of Tet1 and Tet3 mutants. Also see Figure S5G and S5H for the in vitro assay of the catalytic activity of WT and tumor-derived TET2 mutants.

(**E**) Summary of ubiquitylation level, VprBP binding, in vivo and in vitro activity of TET2 leukemia mutants.

See also Figure S5, Table S2.